

**Evidence for $B \rightarrow \eta'\pi$ and improved measurements for $B \rightarrow \eta'K$**

J. Schümann,²² C. H. Wang,²² K. Abe,⁷ I. Adachi,⁷ H. Aihara,⁴³ D. Anipko,¹ K. Arinstein,¹ Y. Asano,⁴⁷ T. Aushev,¹¹ A. M. Bakich,³⁸ V. Balagura,¹¹ E. Barberio,¹⁸ M. Barbero,⁶ A. Bay,¹⁶ I. Bedny,¹ U. Bitenc,¹² I. Bizjak,¹² S. Blyth,²¹ A. Bondar,¹ A. Bozek,²⁴ M. Bračko,^{7,17,12} T. E. Browder,⁶ M.-C. Chang,⁴² P. Chang,²³ Y. Chao,²³ A. Chen,²¹ W. T. Chen,²¹ B. G. Cheon,³ Y. Choi,³⁷ Y. K. Choi,³⁷ A. Chuvikov,³² S. Cole,³⁸ J. Dalseno,¹⁸ M. Danilov,¹¹ M. Dash,⁴⁸ J. Dragic,⁷ A. Drutskoy,⁴ S. Eidelman,¹ D. Epifanov,¹ S. Fratina,¹² N. Gabyshev,¹ T. Gershon,⁷ A. Go,²¹ G. Gokhroo,³⁹ B. Golob,^{50,12} A. Gorišek,¹² H. C. Ha,¹⁴ J. Haba,⁷ T. Hara,²⁹ N. C. Hastings,⁴³ K. Hayasaka,¹⁹ H. Hayashii,²⁰ M. Hazumi,⁷ L. Hinz,¹⁶ T. Hokuue,¹⁹ Y. Hoshi,⁴¹ S. Hou,²¹ W.-S. Hou,²³ Y. B. Hsiung,²³ T. Iijima,¹⁹ A. Imoto,²⁰ K. Inami,¹⁹ A. Ishikawa,⁷ R. Itoh,⁷ M. Iwasaki,⁴³ Y. Iwasaki,⁷ J. H. Kang,⁴⁹ P. Kapusta,²⁴ N. Katayama,⁷ H. Kawai,² T. Kawasaki,²⁶ H. R. Khan,⁴⁴ H. Kichimi,⁷ S. K. Kim,³⁶ S. M. Kim,³⁷ K. Kinoshita,⁴ R. Kulasiri,⁴ R. Kumar,³⁰ C. C. Kuo,²¹ A. Kuzmin,¹ Y.-J. Kwon,⁴⁹ J. S. Lange,⁵ J. Lee,³⁶ T. Lesiak,²⁴ A. Limosani,⁷ D. Liventsev,¹¹ J. MacNaughton,⁹ G. Majumder,³⁹ F. Mandl,⁹ D. Marlow,³² T. Matsumoto,⁴⁵ A. Matyja,²⁴ W. Mitaroff,⁹ H. Miyake,²⁹ H. Miyata,²⁶ Y. Miyazaki,¹⁹ R. Mizuk,¹¹ G. R. Moloney,¹⁸ T. Mori,⁴⁴ T. Nagamine,⁴² I. Nakamura,⁷ E. Nakano,²⁸ M. Nakao,⁷ Z. Natkaniec,²⁴ S. Nishida,⁷ O. Nitoh,⁴⁶ S. Ogawa,⁴⁰ T. Ohshima,¹⁹ T. Okabe,¹⁹ S. Okuno,¹³ S. L. Olsen,⁶ H. Ozaki,⁷ P. Pakhlov,¹¹ H. Palka,²⁴ C. W. Park,³⁷ H. Park,¹⁵ N. Parslow,³⁸ L. S. Peak,³⁸ R. Pestotnik,¹² L. E. Pilonen,⁴⁸ M. Rozanska,²⁴ Y. Sakai,⁷ T. R. Sarangi,⁷ N. Sato,¹⁹ T. Schietinger,¹⁶ O. Schneider,¹⁶ C. Schwanda,⁹ R. Seidl,³³ K. Senyo,¹⁹ M. E. Sevier,¹⁸ M. Shapkin,¹⁰ H. Shibuya,⁴⁰ B. Shwartz,¹ V. Sidorov,¹ A. Sokolov,¹⁰ A. Somov,⁴ N. Soni,³⁰ R. Stamen,⁷ S. Stanič,²⁷ M. Starič,¹² K. Sumisawa,²⁹ S. Suzuki,³⁴ F. Takasaki,⁷ K. Tamai,⁷ N. Tamura,²⁶ M. Tanaka,⁷ G. N. Taylor,¹⁸ Y. Teramoto,²⁸ X. C. Tian,³¹ K. Trabelsi,⁶ T. Tsuboyama,⁷ T. Tsukamoto,⁷ S. Uehara,⁷ T. Uglov,¹¹ K. Ueno,²³ S. Uno,⁷ P. Urquijo,¹⁸ Y. Usov,¹ G. Varner,⁶ K. E. Varvell,³⁸ S. Villa,¹⁶ C. C. Wang,²³ M.-Z. Wang,²³ Y. Watanabe,⁴⁴ E. Won,¹⁴ Q. L. Xie,⁸ A. Yamaguchi,⁴² Y. Yamashita,²⁵ M. Yamauchi,⁷ J. Ying,³¹ Y. Yusa,⁴² C. C. Zhang,⁸ L. M. Zhang,³⁵ Z. P. Zhang,³⁵ V. Zhilich,¹ and D. Zürcher¹⁶

(The Belle Collaboration)

¹*Budker Institute of Nuclear Physics, Novosibirsk*

²*Chiba University, Chiba*

³*Chonnam National University, Kwangju*

⁴*University of Cincinnati, Cincinnati, Ohio 45221*

⁵*University of Frankfurt, Frankfurt*

⁶*University of Hawaii, Honolulu, Hawaii 96822*

⁷*High Energy Accelerator Research Organization (KEK), Tsukuba*

⁸*Institute of High Energy Physics, Chinese Academy of Sciences, Beijing*

⁹*Institute of High Energy Physics, Vienna*

¹⁰*Institute of High Energy Physics, Protvino*

¹¹*Institute for Theoretical and Experimental Physics, Moscow*

¹²*J. Stefan Institute, Ljubljana*

¹³*Kanagawa University, Yokohama*

¹⁴*Korea University, Seoul*

¹⁵*Kyungpook National University, Taegu*

¹⁶*Swiss Federal Institute of Technology of Lausanne, EPFL, Lausanne*

¹⁷*University of Maribor, Maribor*

¹⁸*University of Melbourne, Victoria*

¹⁹*Nagoya University, Nagoya*

²⁰*Nara Women's University, Nara*

²¹*National Central University, Chung-li*

²²*National United University, Miao Li*

²³*Department of Physics, National Taiwan University, Taipei*

²⁴*H. Niewodniczanski Institute of Nuclear Physics, Krakow*

²⁵*Nippon Dental University, Niigata*

²⁶*Niigata University, Niigata*

- ²⁷*Nova Gorica Polytechnic, Nova Gorica*
²⁸*Osaka City University, Osaka*
²⁹*Osaka University, Osaka*
³⁰*Panjab University, Chandigarh*
³¹*Peking University, Beijing*
³²*Princeton University, Princeton, New Jersey 08544*
³³*RIKEN BNL Research Center, Upton, New York 11973*
³⁴*Saga University, Saga*
³⁵*University of Science and Technology of China, Hefei*
³⁶*Seoul National University, Seoul*
³⁷*Sungkyunkwan University, Suwon*
³⁸*University of Sydney, Sydney NSW*
³⁹*Tata Institute of Fundamental Research, Bombay*
⁴⁰*Toho University, Funabashi*
⁴¹*Tohoku Gakuin University, Tagajo*
⁴²*Tohoku University, Sendai*
⁴³*Department of Physics, University of Tokyo, Tokyo*
⁴⁴*Tokyo Institute of Technology, Tokyo*
⁴⁵*Tokyo Metropolitan University, Tokyo*
⁴⁶*Tokyo University of Agriculture and Technology, Tokyo*
⁴⁷*University of Tsukuba, Tsukuba*
⁴⁸*Virginia Polytechnic Institute and State University, Blacksburg, Virginia 24061*
⁴⁹*Yonsei University, Seoul*
⁵⁰*University of Ljubljana, Ljubljana*

We report evidence for exclusive two-body charmless hadronic B meson decays $B \rightarrow \eta'\pi$, and improved measurements of $B \rightarrow \eta'K$. The results are obtained from a data sample of 386×10^6 $B\bar{B}$ pairs collected at the $\Upsilon(4S)$ resonance, with the Belle detector at the KEKB asymmetric energy e^+e^- collider. We measure $\mathcal{B}(B^+ \rightarrow \eta'\pi^+) = [1.76_{-0.62}^{+0.67}(\text{stat})_{-0.14}^{+0.15}(\text{syst})] \times 10^{-6}$ and $\mathcal{B}(B^0 \rightarrow \eta'\pi^0) = [2.79_{-0.96}^{+1.02}(\text{stat})_{-0.34}^{+0.25}(\text{syst})] \times 10^{-6}$. We also report the ratio of $\frac{\mathcal{B}(B^+ \rightarrow \eta'K^+)}{\mathcal{B}(B^0 \rightarrow \eta'K^0)} = 1.17 \pm 0.08(\text{stat}) \pm 0.03(\text{syst})$ and direct CP asymmetries for the charged modes.

PACS numbers: 11.30.Er, 11.30.Hv, 13.20.He, 13.25.Hw, 14.40.Nd, 14.65.Fy

Information on the two-body charmless hadronic B meson decays $B \rightarrow \eta'\pi$ is very limited at present [1]. Measurements of these decay modes can improve the understanding of the flavor-singlet penguin amplitude with intermediate t , c and u quarks [2]. Theoretical predictions for the branching fractions cover the range $(1-17) \times 10^{-6}$ and $(1-8) \times 10^{-6}$ for the charged and neutral decays, respectively [2, 3]. Recently the charged decay was measured by BaBar [5]. In contrast, the channel $B \rightarrow \eta'K$ has been precisely measured [6, 7, 8]. In the Standard Model (SM) the decay is believed to proceed dominantly via gluonic penguin processes [4], and has been evaluated with generalized factorization approaches [9, 10, 11]. The measured branching fractions are, however, significantly larger than these expectations. This has led to speculations that SU(3)-singlet couplings unique to the η' meson or new physics [12, 13] contribute to the amplitude. More precise measurements are needed to constrain the amplitudes and to distinguish between theoretical models. Measurements of ratios of branching fractions, which reduce the effects of form factor uncertainties, are especially useful in this regard.

Additional constraints can be provided by the direct CP asymmetry, $A_{CP} = \frac{\mathcal{B}(\bar{B} \rightarrow \bar{f}) - \mathcal{B}(B \rightarrow f)}{\mathcal{B}(\bar{B} \rightarrow \bar{f}) + \mathcal{B}(B \rightarrow f)}$, where f is the final state and \bar{f} is its CP conjugate. Direct CP violation

in the $B^+ \rightarrow \eta'\pi^+$ mode can be large in the SM [3] while a non-zero value for A_{CP} in $B^+ \rightarrow \eta'K^+$ may require a new physics contribution [4].

In this Letter, we report evidence of $B \rightarrow \eta'\pi$, improved measurements of $B \rightarrow \eta'K$ and a direct CP violation search in the charged B meson decay modes. The results are based on a data sample that contains 386×10^6 $B\bar{B}$ pairs, i.e. 35 times larger than our previous dataset [7], collected with the Belle detector at the KEKB asymmetric-energy e^+e^- (3.5 on 8 GeV) collider [14]. KEKB operates at the $\Upsilon(4S)$ resonance ($\sqrt{s} = 10.58$ GeV).

The Belle detector is a large-solid-angle magnetic spectrometer that consists of a silicon vertex detector, a 50-layer central drift chamber (CDC), an array of aerogel threshold Čerenkov counters (ACC), a barrel-like arrangement of time-of-flight scintillation counters (TOF), and an electromagnetic calorimeter comprised of CsI(Tl) crystals located inside a superconducting solenoid coil that provides a 1.5 T magnetic field. An iron flux-return located outside of the coil is instrumented to detect K_L^0 mesons and to identify muons. The detector is described in detail elsewhere [15]. Two inner detector configurations are used. A 2.0 cm beampipe and a 3-layer silicon vertex detector is used for the first sample of 152×10^6

$B\bar{B}$ pairs (Set I), while a 1.5 cm beampipe, a 4-layer silicon detector and a small-cell inner drift chamber are used to record the remaining 234×10^6 $B\bar{B}$ pairs (Set II) [16].

Charged hadrons are identified by combining information from the CDC (dE/dx), ACC and TOF systems. Both kaons and pions are selected with an efficiency of about 86%. Tighter criteria are applied to the pion candidate in $B^+ \rightarrow \eta' \pi^+$, resulting in an efficiency (kaon misidentification probability) of about 77% (4%).

The η' mesons are reconstructed via two decay chains: $\eta' \rightarrow \eta \pi^+ \pi^-$ (with $\eta \rightarrow \gamma \gamma$) and $\eta' \rightarrow \rho^0 \gamma$. We reconstruct π^0 , ρ^0 , η , η' and K_S^0 candidates using the mass windows given in Table I. In addition, we require the following. All photons are required to have an energy of at least 50 MeV, photons from η' in $\eta' \rightarrow \rho^0 \gamma$ of at least 100 MeV. The transverse momenta of π^\pm for ρ^0 candidates have to be greater than 200 MeV/ c . The vertex of the $K_S^0 \rightarrow \pi^+ \pi^-$ has to be displaced from the interaction point and the K_S^0 momentum direction must be consistent with its flight direction. For $B^0 \rightarrow \eta' \pi^0$, we require $|h_{\pi^0}| = \frac{E(\gamma_1) - E(\gamma_2)}{E(\gamma_1) + E(\gamma_2)} < 0.95$ (0.6) for $\eta' \rightarrow \eta \pi^+ \pi^-$ ($\eta' \rightarrow \rho^0 \gamma$), where $E(\gamma_{1,2})$ is the energy of the two π^0 decay photons. Similarly, we require $|h_\eta| < 0.85$.

TABLE I: Mass windows to reconstruct intermediate states.

mode	mass window (MeV/ c^2)
$\pi^0 \rightarrow \gamma \gamma$	[118,150] $\pm 2.5\sigma$
$\rho^0 \rightarrow \pi^+ \pi^-$	[550,870] —
$\eta \rightarrow \gamma \gamma$	[500,570] $+2.5\sigma/-3.3\sigma$
$\eta' \rightarrow \eta \pi^+ \pi^-$ (in $\eta' K$)	[945,970] $\pm 3.4\sigma$
$\eta' \rightarrow \rho^0 \gamma$ (in $\eta' K$)	[935,975] $\pm 3\sigma$
$\eta' \rightarrow \eta \pi^+ \pi^-$ (in $\eta' \pi$)	[950,965] $\pm 2.5\sigma$
$\eta' \rightarrow \rho^0 \gamma$ (in $\eta' \pi$)	[941,970] $\pm 2.5\sigma$
$K_S^0 \rightarrow \pi^+ \pi^-$	[485,510] $\pm 3\sigma$

B meson candidates are reconstructed combining an η' meson with a pion or kaon candidate. Two kinematic variables are used to extract the B meson signal: the energy difference, $\Delta E = E_B - E_{\text{beam}}$, and the beam-energy constrained mass, $M_{\text{bc}} = \sqrt{E_{\text{beam}}^2/c^4 - (P_B/c)^2}$, where E_{beam} is the beam energy and E_B and P_B are the reconstructed energy and momentum of the B candidate in the $\Upsilon(4S)$ rest frame. Events satisfying the requirements $M_{\text{bc}} > 5.2$ GeV/ c^2 and $|\Delta E| < 0.25$ GeV are selected for further analysis. Around 10% of these events have multiple B candidates. Among these candidates the one with the smallest $\chi_{\text{vtx}}^2 + \chi_{\eta'}^2$ is selected, where χ_{vtx}^2 is a goodness of vertex fit for all charged particles and $\chi_{\eta'}^2 = [(M(\eta') - m_{\eta'}/\sigma_{\eta'})^2]$, where $M(\eta')$ is the η' candidate mass, $m_{\eta'}$ is the nominal mass of the η' and $\sigma_{\eta'} = 8$ MeV/ c^2 is the width of the η' mass distribution.

Several event shape variables (defined in the center of mass frame) are used to distinguish the spherical $B\bar{B}$ topology from the jet-like $q\bar{q}$ continuum events. The thrust angle θ_T is defined as the angle between the η' mo-

mentum direction and the thrust axis formed by all particles not belonging to the reconstructed B meson. Jet-like events tend to peak near $|\cos \theta_T| = 1$, while spherical events have a uniform distribution. The requirement $|\cos \theta_T| < 0.9$ is applied prior to all other event topology selections.

Additional continuum suppression is obtained by using modified Fox-Wolfram moments [17] and the angle θ_B between the flight direction of the reconstructed B candidate and the beam axis. A Fischer discriminant (\mathcal{F}) [18] is formed from a linear combination of $\cos \theta_T$, S_\perp and five modified Fox-Wolfram moments. S_\perp is the ratio of the scalar sum of the transverse momenta of all tracks outside a 45° cone around the η' direction to the scalar sum of their total momenta. These variables are then combined to form an event-topology likelihood function \mathcal{L}_s ($\mathcal{L}_{q\bar{q}}$), where s ($q\bar{q}$) represents signal (continuum background). We include the quality of the B flavor tagging of the accompanying B meson to improve continuum rejection. The standard Belle B tagging package [19] is used, which gives the B flavor and a tagging quality r ranging from zero for no flavor to unity for unambiguous flavor assignment. The data is divided into three r regions. Signal-like events are selected by applying likelihood ratio $\mathcal{R} = \mathcal{L}_s / (\mathcal{L}_s + \mathcal{L}_{q\bar{q}})$ requirements optimized on MC events in the three r regions separately. For channels with an $\eta' \rightarrow \rho^0 \gamma$ decay an additional variable $\theta_{\mathcal{H}}$, which is the angle between the η' momentum and the direction of one of the decay pions in the ρ^0 rest frame, is included for better signal-background separation.

The branching fractions are extracted using extended unbinned maximum-likelihood fits to two-dimensional ($\Delta E, M_{\text{bc}}$) distributions for the $\eta' \rightarrow \eta \pi^+ \pi^-$ and $\eta' \rightarrow \rho^0 \gamma$ sub-decays simultaneously. The extended likelihood function used is:

$$L(N_S, N_{B_j}) = \frac{e^{-(N_S + \sum_j N_{B_j})}}{N!} \prod_{i=1}^N \left[N_S P_S(\Delta E_i, M_{\text{bc}_i}) + \sum_j N_{B_j} P_{B_j}(\Delta E_i, M_{\text{bc}_i}) \right] \quad (1)$$

where N_S (N_{B_j}) is the number of signal events (background events of source j) with probability density functions (PDFs) P_S (N_{B_j}) and the index i runs over the total number of events $N = N_S + \sum_j N_{B_j}$.

The reconstruction efficiencies are determined from signal MC samples, using the EvtGen package [20] with final state radiation simulated by the PHOTOS package [21]. The efficiencies are calculated separately for both Set I and Set II. The absolute efficiency for Set II is typically about 0.5% larger than for Set I (for efficiencies averaged over the two sets see Table II). The signal yield is expressed as $N_S = \epsilon_1 N_{(B\bar{B})_1} \mathcal{B} + \epsilon_2 N_{(B\bar{B})_2} \mathcal{B}$, where \mathcal{B} is the signal branching fraction, and ϵ_i and $N_{(B\bar{B})_i}$ are the efficiency and the number of $B\bar{B}$ pairs for Set I

and Set II. The numbers of B^+B^- and $B^0\bar{B}^0$ pairs are assumed to be equal. Correction factors due to differences between data and MC are included for the charged track identification and photon, π^0 and η reconstruction, resulting in an overall correction factor of ≈ 0.9

The PDF shapes for each contribution are determined by MC studies. The signal shapes for ΔE and M_{bc} are assumed to be independent. We model the signal using a Gaussian with an exponential tail (Crystal Ball function) [22] plus a Gaussian for ΔE and a Gaussian with an exponential tail for M_{bc} .

We consider four types of backgrounds separately in the fit: continuum, $b \rightarrow c$ and two types of charmless decays. Continuum background is modeled by a first or second order polynomial for ΔE and an ARGUS function [23] for M_{bc} . Charmless B decays and $b \rightarrow c$ backgrounds are modeled with smoothed two-dimensional histograms. The contributions from charmless B decays are split into two components, one for the decay with the largest contribution and one for all other charmless decays. For $B^+ \rightarrow \eta'K^+$, the dominant mode, which is modeled separately is $B \rightarrow \eta'K^*$; for $B^0 \rightarrow \eta'K^0$ it is $B \rightarrow \rho^0K_S^0$; for $B^0 \rightarrow \eta'\pi^0$ it is $B \rightarrow \rho\rho$; and for $B^+ \rightarrow \eta'\pi^+$ it is the $B^+ \rightarrow \eta'K^+$ feed-down. The feed-down in $B^+ \rightarrow \eta'\pi^+$ is modeled with the same PDFs as used for the $\eta'K^+$ signal, shifted and with a corrected width in ΔE .

The continuum shape parameters are allowed to float in all modes. The signal mean and width parameters are free for the kaonic modes. For the $B^+ \rightarrow \eta'\pi^+$ mode these parameters are fixed to the values obtained from the charged kaon mode. For $\eta' \rightarrow \eta\pi^+\pi^-$ modes our background MC studies show that no contributions from $b \rightarrow c$ decays are expected. The sizes of background contributions other than continuum are constrained to the values expected from MC studies. The $B^+ \rightarrow \eta'K^+$ component in the $B^+ \rightarrow \eta'\pi^+$ decay is fixed by the branching fraction of $B^+ \rightarrow \eta'K^+$ as measured here and the probability of kaons faking pions. A simultaneous fit with the branching fraction and the charge asymmetry as common parameters is used. The resulting projection plots are shown in Fig. 1. The reconstruction efficiencies and fit results are given in Table II.

We find first evidence for the neutral decay:

$$\mathcal{B}(B^0 \rightarrow \eta'\pi^0) = [2.79_{-0.96}^{+1.02}(\text{stat})_{-0.34}^{+0.25}(\text{syst})] \times 10^{-6},$$

and evidence for the charged decay:

$$\mathcal{B}(B^\pm \rightarrow \eta'\pi^\pm) = [1.76_{-0.62}^{+0.67}(\text{stat})_{-0.14}^{+0.15}(\text{syst})] \times 10^{-6}.$$

The ratio of the branching fractions for charged and neutral $B \rightarrow \eta'K$ decays is found to be $1.17 \pm 0.08 \pm 0.03$, assuming equal production of B^+B^- and $B^0\bar{B}^0$. The charge asymmetries for the $B^+ \rightarrow \eta'\pi^+$ and $B^+ \rightarrow \eta'K^+$ decay modes, listed in Table II, show no significant deviation from zero.

Systematic errors are estimated with various high statistics data samples. The dominant sources are the uncertainties of the reconstruction efficiency of charged tracks (3–4%), the uncertainties in the reconstruction efficiencies for η mesons and photons (3–6%) and the uncertainty of the PDF shapes and parameters (1–9%). Other systematic uncertainties arise from the K feed-down in $B^+ \rightarrow \eta'\pi^+$ ($\approx 2\%$), the differences between data and MC for ΔE and M_{bc} in $B^+ \rightarrow \eta'\pi^+$ ($\approx 4\%$), the K_S reconstruction efficiency uncertainty (4%), the uncertainty of the sub-decay branching fractions as given by the Particle Data Group (PDG) [24] (1.5%), the number of $B\bar{B}$ mesons produced (1%), the efficiency differences due to signal simulation by different MC generators (1.4%), the uncertainty in the efficiency (1%) and the uncertainty from particle identification (0.7%). The errors are added in quadrature and we find the systematic errors to be $\pm 5.4\%$, $\pm 7.3\%$, $_{-7.7}^{+8.5}\%$ and $_{-12.1}^{+8.8}\%$ for $B^+ \rightarrow \eta'K^+$, $B^0 \rightarrow \eta'K^0$, $B^+ \rightarrow \eta'\pi^+$ and $B^0 \rightarrow \eta'\pi^0$ decays, respectively. For the charge asymmetry, efficiency based systematic errors cancel out. We estimate the possible detector bias on A_{CP} from the charge asymmetry of the continuum background in the $B^+ \rightarrow \eta'K^+$ sample which is obtained simultaneously from the fit. We assign 0.02 as systematic error both for $B^+ \rightarrow \eta'K^+$ and $\eta'\pi^+$. Other contributions from fitting and normalization together result in a systematic error of 0.003 for $B^+ \rightarrow \eta'K^+$. For $B^+ \rightarrow \eta'\pi^+$ the uncertainties from PDF shapes and feed-down contributions add up to $_{-0.04}^{+0.03}$.

The significance of the $B^+ \rightarrow \eta'\pi^+$ yield is 3.2σ , which is calculated as $\sigma = \sqrt{2 \ln(\mathcal{L}_{\text{max}}/\mathcal{L}_0)}$, where \mathcal{L}_{max} and \mathcal{L}_0 denote the maximum likelihood value and the likelihood value at zero branching fraction, respectively. The systematic error is included in the significance calculation. For $B^0 \rightarrow \eta'\pi^0$ the corresponding significance with systematics is 3.1σ .

In summary, evidence for $B \rightarrow \eta'\pi$ with greater than 3σ significance is found and improved measurements for the charged and neutral $B \rightarrow \eta'K$ decays are reported. The measured branching fractions of $B \rightarrow \eta'K$ decays supersede our previous results [7] and are consistent with the measurements of CLEO [6] and BaBar [5]. No charge asymmetry is observed in the decay modes $B^+ \rightarrow \eta'K^+$ and $B^+ \rightarrow \eta'\pi^+$.

We thank the KEKB group for excellent operation of the accelerator, the KEK cryogenics group for efficient solenoid operations, and the KEK computer group and the NII for valuable computing and Super-SINET network support. We acknowledge support from MEXT and JSPS (Japan); ARC and DEST (Australia); NSFC and KIP of CAS (contract No. 10575109 and IHEP-U-503, China); DST (India); the BK21 program of MOEHRD, and the CHEP SRC and BR (grant No. R01-2005-000-10089-0) programs of KOSEF (Korea); KBN (contract No. 2P03B 01324, Poland); MIST (Russia); ARRS (Slovenia); SNSF (Switzerland); NSC and MOE (Tai-

TABLE II: Signal efficiencies (ϵ_{tot}) with sub-decay branching fractions included and averaged for Set I and Set II for $\eta' \rightarrow \eta\pi^+\pi^-$ and $\eta' \rightarrow \rho^0\gamma$, total signal yields N_S , branching fractions \mathcal{B} , signal asymmetries A_{CP} , and significances σ . The first errors are statistical and the second (if given) are systematic errors.

	$B^+ \rightarrow \eta' K^+$	$B^0 \rightarrow \eta' K^0$	$B^+ \rightarrow \eta' \pi^+$	$B^0 \rightarrow \eta' \pi^0$
$\epsilon_{\text{tot}}(\eta' \rightarrow \eta\pi^+\pi^-)$ [%]	4.31 ± 0.03	1.19 ± 0.03	2.84 ± 0.03	1.72 ± 0.02
$\epsilon_{\text{tot}}(\eta' \rightarrow \rho^0\gamma)$ [%]	2.78 ± 0.04	1.07 ± 0.04	2.89 ± 0.04	1.72 ± 0.03
N_S	1895.7 ± 59.5	515.3 ± 31.7	39.0 ± 13.2	35.8 ± 12.7
$\mathcal{B}[10^{-6}]$	$69.2 \pm 2.2 \pm 3.7$	$58.9_{-3.5}^{+3.6} \pm 4.3$	$1.76_{-0.62-0.14}^{+0.67+0.15}$	$2.79_{-0.96-0.34}^{+1.02+0.25}$
A_{CP}	$0.028 \pm 0.028 \pm 0.021$	—	$0.20_{-0.36}^{+0.37} \pm 0.04$	—
σ	> 10	> 10	3.2	3.1

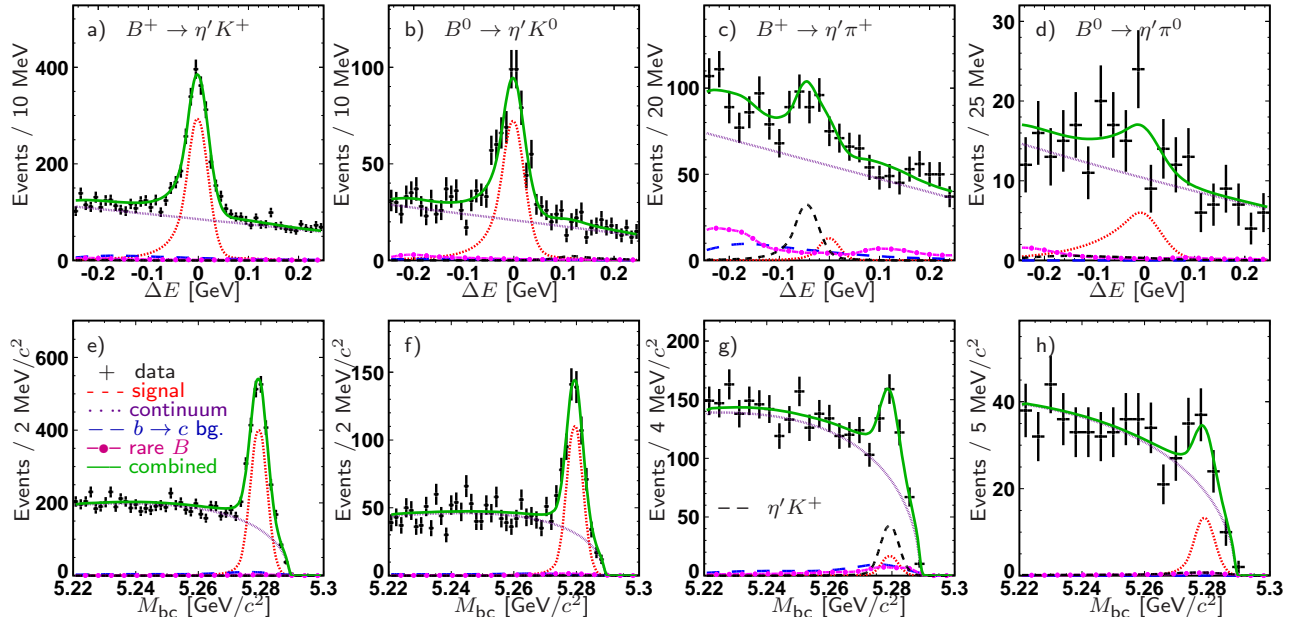


FIG. 1: ΔE and M_{bc} distributions for $B^+ \rightarrow \eta' K^+$ (a, e), $B^0 \rightarrow \eta' K^0$ (b, f), $B^+ \rightarrow \eta' \pi^+$ (c, g) and $B^0 \rightarrow \eta' \pi^0$ (d, h), respectively, for the region $M_{bc} > 5.27 \text{ GeV}/c^2$ and $-0.12 \text{ GeV} < \Delta E < 0.08 \text{ GeV}$ for $B^0 \rightarrow \eta' \pi^0$ and $-0.1 \text{ GeV} < \Delta E < 0.06 \text{ GeV}$ for all others.

wan); and DOE (USA).

[1] Throughout this paper, the inclusion of the charge conjugate mode decay is implied unless otherwise stated.
[2] C. W. Chiang, M. Gronau, J. L. Rosner and D. A. Suprun, Phys. Rev. D **70** (2004) 034020.
[3] H. K. Fu, X. G. He and Y. K. Hsiao, Phys. Rev. D **69** (2004) 074002.
[4] Y. Grossman and M. P. Worah, Phys. Lett. B **395** (1997) 241.
[5] B. Aubert *et al.* (BaBar Collaboration), Phys. Rev. Lett. **95** (2005) 131803.
[6] S. J. Richichi *et al.* (CLEO Collaboration), Phys. Rev. Lett. **85** (2000) 520.
[7] K. Abe *et al.* (Belle Collaboration), Phys. Lett. B **517** (2001) 309.
[8] B. Aubert *et al.* (BaBar Collaboration), Phys. Rev. Lett. **94** (2005) 191802.

[9] A. A. Petrov, Phys. Rev. D **58** (1998) 054004.
[10] A. Ali, G. Kramer, and C. D. Lu, Phys. Rev. D **58** (1998) 094009.
[11] D.-S. Du, C. S. Kim, and Y.-D. Yang, Phys. Lett. B **426** (1998) 133.
[12] Z. J. Xiao, W. J. Li, L. B. Guo, and G. R. Lu, Mod. Phys. Lett. A **16** (2001) 441.
[13] S. Khalil and E. Kou, Phys. Rev. Lett. **91** (2003) 241602.
[14] S. Kurokawa and E. Kikutani, Nucl. Instr. and Meth. A **499** (2003) 1, and other papers included in this volume.
[15] A. Abashian *et al.* (Belle Collab.), Nucl. Instr. and Meth. A **479** (2002) 117.
[16] Y. Ushiroda (Belle SVD2 Group), Nucl. Instr. and Meth. A **511** (2003) 6.
[17] The Fox-Wolfram moments were introduced in G. C. Fox and S. Wolfram, Phys. Rev. Lett. **41** (1978) 1581. The Fisher discriminant used by Belle, based on modified Fox-Wolfram moments (SFW), is described in K. Abe *et al.* (Belle Collab.), Phys. Rev. Lett. **87** (2001) 101801.
[18] R. A. Fisher, Annals of Eugenics **7** (1936) 179.
[19] H. Kakuno *et al.*, Nucl. Instr. and Meth. A **533** (2004) 516.

- [20] D. J. Lange, Nucl. Instr. and Meth. A **462** (2001) 152.
- [21] E. Barberio and Z. Was, Comp. Phys. Comm. **79** (1994) 291.
- [22] J. E. Gaiser *et al.* (Crystal Ball Collaboration) Phys. Rev. D **34** (1986) 711.
- [23] H. Albrecht *et al.* (ARGUS Collaboration), Phys. Lett. B **241** (1990) 278.
- [24] S. Eidelman *et al.* (Particle Data Group), Phys. Lett. B **592** (2004) 1.